Chemical Science

ROYAL SOCIETY OF CHEMISTRY

EDGE ARTICLE

View Article Online
View Journal | View Issue

Check for updates

Cite this: *Chem. Sci.*, 2021, **12**, 5152

All publication charges for this article have been paid for by the Royal Society of Chemistry

Received 2nd February 2021
Accepted 20th February 2021

DOI: 10.1039/d1sc00642h

rsc.li/chemical-science

The ortho effect in directed C–H activation†

Balázs L. Tóth, *[a] Anna Monory,[a] Orsolya Egyed,[b] Attila Domján,[b] Attila Bényei,[c] Bálint Szathury,[d] Zoltán Novák *[a] and András Stirling *[be]

The success of transition metal-catalysed *ortho*-directed C–H activation is often plagued by the effects of undesirable interactions between the directing group (DG) and other groups introduced into the aromatic core of the substrate. In particular, when these groups are in neighbouring positions, their interactions can affect profoundly the efficacy of the C–H activation by transition metals. In this work we introduce a simple *substrate-only-based* model to interpret the influence of steric hindrance of a group in *ortho* position to the DG in directed *ortho*-C–H bond activation reactions, and coined the term Ortho Effect (OE) for such situations. We consider simple descriptors such as torsion angle and torsional energy to predict and explain the reactivity of a given substrate in directed C–H activation reactions. More than 250 examples have been invoked for the model, and the nature of the ortho effect was demonstrated on a wide variety of structures. In order to guide organic chemists, we set structural and energetic criteria to evaluate *a priori* the efficiency of the metalation step which is usually the rate-determining event in C–H activations, *i.e.* we provide a simple and general protocol to estimate the reactivity of a potential substrate in C–H activation. For borderline cases these criteria help set the minimum reaction temperature to obtain reasonable reaction rates. As an example for the practical applicability of the model, we performed synthetic validations *via* palladium-catalysed 2,2,2-trifluoroethylation reactions in our lab. Furthermore, we give predictions for the necessary reaction conditions for several selected DGs.

Introduction

C–H activation reactions became one of the most important transformations in modern synthetic organic chemistry, which enable the cleavage of the inert aromatic C–H bond and its direct substitution with different carbon-containing functional groups such as the alkynyl, aryl, alkenyl, alkyl or acyl group with the aid of catalytic amounts of transition metals such as Pd, Rh, Ru, Co, Ir, Ni, Mn, and Cu.[1] In aromatic compounds, there are many hydrogen atoms in similar chemical environments, which can raise problems of regioselectivity. However, the presence of a directing group (DG) in the aromatic core allows selective metalation in the *ortho*, *meta* or even in *para* positions.[2–4] The efficacy of these processes critically depends on the C–H bond breaking and the formation of the metalated complex containing a carbon–metal bond, which is in many cases the rate limiting step of the catalytic cycle. This step could take place through various mechanistic scenarios such as electrophilic palladation, oxidative addition or CMD/AMLA mode,[5] resulting in cyclometalated complexes. The electronic and steric properties of the substrates have a strong influence on the C–H activation step, on the stability of the metallacycle intermediates and on the synthetic outcome of the overall transformation. The beneficial electronic and steric properties could result in efficient functionalisations under mild reaction conditions, but often structural variations can prevent the C–H activation even under more forced reaction conditions. As an electrophilic metalation mechanism, the electronic effects on C–H activation reactions are well-understood.[6] However, the more complex and less foreseeable effects of steric conflicts have remained often elusive without a general, thorough explanation. There is a very frequent situation in *ortho* C–H activation, when the substituent is located in the aromatic core at one of the *ortho* positions compared to the DG. For this particular situation we coin the term Ortho Effect (OE) referring to the steric influence of this group in *ortho* position to the DG on the

[a]*ELTE "Lendület" Catalysis and Organic Synthesis Research Group, Faculty of Science, Institute of Chemistry, Eötvös Loránd University, Pázmány Péter Sétány. 1/A, H-1117 Budapest, Hungary. E-mail: tothb@zng.elte.hu; novakz@elte.hu*

[b]*Research Centre for Natural Sciences, Eötvös Loránd Research Network, Magyar Tudósok Körútja 2, H-1117 Budapest, Hungary. E-mail: stirling.andras@ttk.hu*

[c]*Department of Physical Chemistry, University of Debrecen, Egyetem Tér 1, H-4032 Debrecen, Hungary*

[d]*Department of Chemistry, University of Cambridge, Lensfield Rd, Cambridge CB2 1EW, UK*

[e]*Department of Chemistry, Eszterházy Károly University, Leányka u. 6, H-3300 Eger, Hungary*

† Electronic supplementary information (ESI) available: General reaction conditions, characterization and NMR spectra, full interactive database as a supplementary XLSX (MS Excel) file, zip compressed XYZ files containing atomic coordinates of substrates and CIF files for XRD coordinates. CCDC deposition numbers are 2044698–2044703 for **4-Pd**, **8-Pd**, **9-Pd**, **11-Pd**, **44**, and **45**, respectively. For ESI and crystallographic data in CIF or other electronic format see DOI: 10.1039/d1sc00642h

Open Access Article. Published on 02 March 2021. Downloaded on 9/25/2023 2:55:44 PM.
This article is licensed under a Creative Commons Attribution-NonCommercial 3.0 Unported Licence.

© 2021 The Author(s). Published by the Royal Society of Chemistry

Open Access Article. Published on 02 March 2021. Downloaded on 9/25/2023 2:55:44 PM.
This article is licensed under a Creative Commons Attribution-NonCommercial 3.0 Unported Licence.

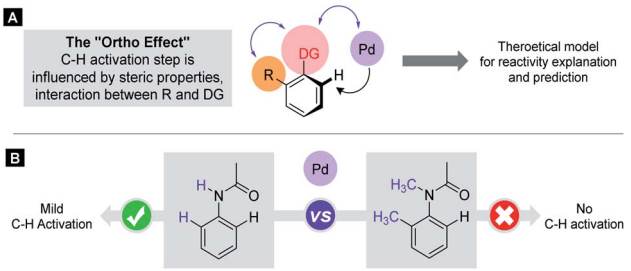

Fig. 1 The substrate-dependent OE in Pd catalysed C–H activation. (A) General representation of OE. (B) Demonstration of OE with anilides.

metalation of C–H bond in the other *ortho* position of the aromatic substrate (Fig. 1A). As an example, the significant difference between the reactivity of acetanilide and 2-methyl-*N*-methylacetanilide provides a clear example for OE. While acetanilide can be functionalized in the *ortho* positions in various C–H activation reactions even under mild conditions, the functionalisation of 2-methyl-*N*-methylacetanilide remained unprecedented (Fig. 1B), which can be attributed to steric effects (additional examples representing situations between the two extremes are presented in the ESI†).[7–17]

Generally, the steric interactions can be very complex. Small variations in their pattern can often lead to considerable changes in reactivities, hence their effects are difficult to predict.[18] OE is easy to understand intuitively, but to the best of our knowledge, so far, no attempt has been made to identify, define and quantify its extent. On the other hand, a large body of empirical experience is available in a number of publications where the role of OE can be presumed.[7–17] In view of this we raise the following questions:

Can a suitable, qualitative model of OE be devised by exploiting the available experimental data to establish correlation between reactivity and the relevant properties of the substrates?

Can simple descriptors be identified to predict the OE based on the properties of the substrates and the experimental results?

Characterizing the reactivity requires mechanistic insight transferable within a wide range of analogous reactions. In *ortho*-directed C–H activations the C–H bond breaking and the formation of the carbon–metal bond is a necessary and sufficient prerequisite of the successful *ortho*-metalation. Often this step is the kinetic bottleneck in these reactions.[1i] Hence, we focus on this step determining the rate and selectivity of the whole reaction to grasp the efficiency of the C–H activations. It is important to note that the isolation of metallic species as intermediates in the C–H activation step is a frequently used experimental strategy to obtain more detailed mechanistic insight into the catalytic transformations.

Assessing the reactivity requires large number of comparable and reliable data for both extremes (high and low) of reactivities. Although numerous examples have been disclosed for diverse substrate functionalisation using transition metal catalysed C–H bond activation under various reaction conditions,[1] the compilation of the data is far from straightforward. The effects of the limiting structural molecular motifs are typically not scrutinized and the unsuccessful experiments are seldom reported. In the absence of details, the failed reaction setups are hidden to the public which hampers mechanistic interpretations.

Correlating selected descriptors with desired chemical properties has been a successful design strategy in various fields of chemistry, and especially in catalysis.[19] In the present context we seek simple structural or energetic parameters of the substrate which correlate with the reactivities of the substrate in the carbon–metal bond formation step. For quantifying reactivities we need to select parameters representing the applied conditions of the reaction leading to the metallacycle formation (such as temperature or reaction time) and values representing the efficiency of the reactions (conversions or yields). This approach warrants some additional thoughts: we envision in principle two viable directions to follow:

(I) a *reaction-based* approach where we compute reaction routes for selected metals and ligands and make predictions on the basis of the results;

(II) a *substrate-only-based* approach where suitably selected properties of the substrate are used to predict reactivities.

The former approach has the advantage of being accurate whereas it has the disadvantage that the more specific (regarding ligand and metal selection) and accurate the strategy, necessarily the less general its scope is and the less general is the model it offers. In contrast, the substrate-only-based model is less accurate but it can be far wider in scope. We think that a substrate-only based model can address reactivity issues in typical synthetic problems more efficiently than a costly approach and the practice appreciates it more favourably.

In this study therefore we aimed to develop a theoretical substrate-only-based model to investigate the OE in Pd catalysed *ortho* C–H activation reaction with the analysis of a large number of available substrates. DFT calculations provided simple descriptors (torsional angles and torsional energies) which are shown here to perform surprisingly well to capture the experimentally observed reactivities for a large set (>250) of substrates. Our goal was to show how to assess the reactivity of a potential substrate using these descriptors and how to obtain a preliminary estimation of the reaction temperature in advance. In particular, we wish to demonstrate here that with this simple model:

(I) one can decide in a binary yes/no fashion whether a reaction is expected;

(II) in borderline cases the model helps to set the reaction temperature for a likely successful reaction;

(III) one can assess the regioselectivity when competing sites are available;

(IV) one can predict the outcome for single *vs.* double *ortho*-functionalisation reactions.

Results and discussion

Computational details

The calculations for constructing the model require optimizations of substrate conformers. The calculations have been

Open Access Article. Published on 02 March 2021. Downloaded on 9/25/2023 2:55:44 PM.
This article is licensed under a Creative Commons Attribution-NonCommercial 3.0 Unported Licence.

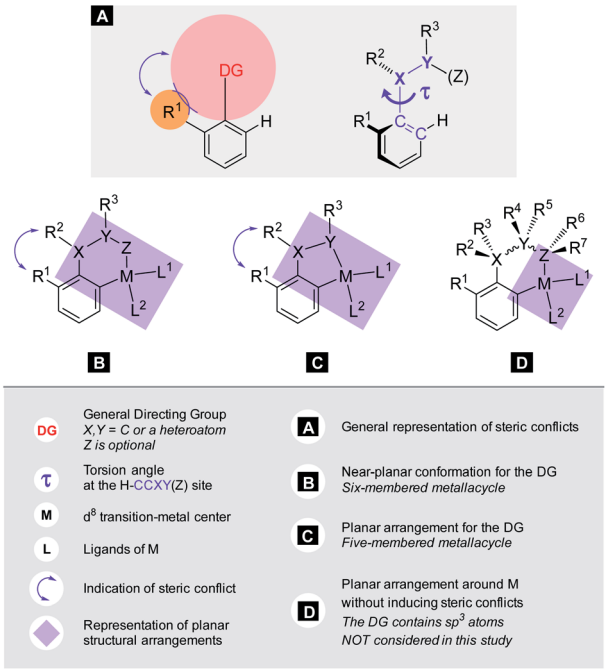

Scheme 1 Conformational changes during *ortho*-cyclometalation on an aryl substrate.

performed using the Gaussian 09 software package.[20] The ωB97XD functional[21] with the 6-311++G** basis set has been employed for the geometry optimizations. Full optimizations have been done for all substrates and then a restricted optimization was performed where the chelating chain was forced to be in the plane of the ring by constraining the dihedral angle (τ) to be zero (Scheme 1) without any metal catalyst (M). Solvent effects were not included in the calculations. We assume that the solvents, employed in the experiments where yields were taken, are properly selected (during the optimization studies) for the ideal reactivity of the substrates and the solvents have similar effects on the equilibrium and planar conformers of a given substrate. In this study we will approximate the rotational Gibbs free energy (ΔG_{rot}) by the computed Kohn–Sham energy difference of the equilibrium and constrained geometries, where the conformational angle (τ) is set to 0° (Scheme 1) and neglect the entropy, vibrational and zero-point energy differences between the equilibrium and constrained structures. We note that when formation of a six-membered metallacycle is expected all the three atoms of DG are forced to be in-plane with the aromatic ring requiring two dihedral angles to be 0°. In the following we will use either the equilibrium dihedral angle τ, or the term ΔG_{rot} when discussing the effect of steric hindrance between DG and *ortho* groups. In addition, we also express ΔG_{rot} in *RT* units (standardized ΔG_{rot}; $\Delta G'_{rot} = \Delta G_{rot}/RT$), *i.e.* we can compare torsional energies at different temperatures.

Theory for C–H activation with d^8 metals

Our objective is to find suitable descriptors for the steric conflicts between DG and the *ortho*-substituents of the aromatic substrate. In principle, a number of structural parameters could be used to quantify the steric bulks of the ligands in question such as distances between selected atoms, specifically defined volumes or dimensional parameters.[18a] Still, simplicity and chemical intuition suggest that the equilibrium value of τ or the corresponding torsional energy ΔG_{rot} can be suitable simple quantities to predict the effectiveness of *ortho*-functionalisation. In the following we verify this hypothesis, define its limitations and show examples how this concept can be efficiently exploited.

Previous calculations and measurements have shown that after the coordination of the DG's heteroatom to M, the intermediates feature a planar ligand arrangement around M which is coplanar with the aryl group.[15] Such a situation can arise for d^8 metal centres (Scheme 1). This planarity represents an important constraint for chelate formation: the bond between M and DG must be coplanar with the aryl ring. However, this often comes at the prize of steric conflicts between groups that are not participating in the formation of the metallacycle as shown in Scheme 1. This is a crucial issue when the formation of the metallacycle is the rate-determining step because in such cases the efficiency of the whole functionalisation reaction is strongly dependent on the extent of the steric repulsion induced by the formation of the metallacycle in the C–H activation stage as explained in Fig. 2. In this spirit, the activation barrier can be hypothetically divided into two components: an energy term for the necessary conformational change of DG for chelation (ΔG_{rot}) and the energy investment for the rest of the chemical changes ($\Delta G^{\#}_{chem}$) as pictorially shown in Fig. 2. Clearly, the smaller the energy for the conformational change (ΔG_{rot}) is for a given $\Delta G^{\#}_{chem}$, the faster the reaction is as the total activation barrier ($\Delta G^{\#}$) is smaller.

We note that similar theoretical decompositions have been proposed earlier and have been employed with great success.[22] In these methods the activation energy is expressed in terms of distortion strains of the reactants (bond elongations, bond angle

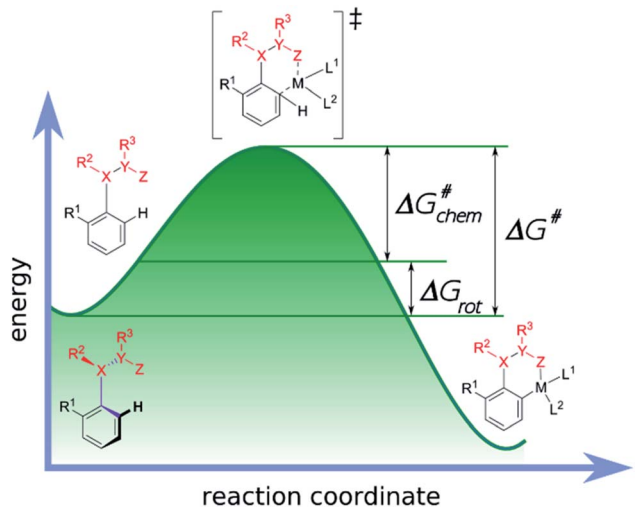

Fig. 2 Energy profile of a typical transition-metal catalysed aryl C–H activation and its decomposition into two terms: the rotation (ΔG_{rot}) and the chemical terms ($\Delta G^{\#}_{chem}$).

© 2021 The Author(s). Published by the Royal Society of Chemistry

Open Access Article. Published on 02 March 2021. Downloaded on 9/25/2023 2:55:44 PM.
This article is licensed under a Creative Commons Attribution-NonCommercial 3.0 Unported Licence.

and torsional angle variations) and the interaction energy between the strained reactants. The main difference in our approach is that we seek parameters that are characteristic of the original substrate alone without invoking any metal catalyst, *i.e.* we focus on the equilibrium properties of the substrates only.

This is why the activation barrier is dissected to an energy term representative of the initial reactant (ΔG_{rot}) whereas the rest of the contributions to the barrier (*e.g.* additional strain and interaction energy components) are included in the term $\Delta G^{\#}_{chem}$. It is also important to note that this division implies the planarity of the TS-s. However, this assumption is only approximately valid, because the TS is not necessarily fully planar, hence a small portion of energy necessary to reach full planarity might be covered by the reaction heat liberated after the TS. On the other hand ΔG_{rot} is a well-defined quantity for the substrates alone which is an advantageous factor for standardization of the model.

This decomposition can establish a conceptual model where a simple structural or energetic property of the substrate can predict the reaction performance in *ortho*-functionalisation. The goal is therefore to assess the extent to which τ or ΔG_{rot} alone can be used to make prediction for the *ortho*-functionalisation without additional computations (*e.g.* transition state [TS] calculations).

The first step along this line is to verify that the energy to constrain the DG into the necessary planar conformation for chelate formation (ΔG_{rot}) indeed depends on the dihedral angle τ in a systematic fashion. For this we have considered the whole set of substrates curated for this study featuring an aromatic core suitable for the *ortho*-substitution. For many of these molecules experimental data are available but we have also included those which have not yet been employed in *ortho*-functionalisations. The full database is presented as part of the ESI† (Full Interactive Database). Fig. 3 displays the variation of ΔG_{rot} as a function of τ calculated for each substrate.

It is seen that there is an apparent correlation between τ and the torsional energy (*i.e.* ΔG_{rot} and τ are not independent parameters). At large angles however we can see larger scattering. In particular, there are cases where the distortion requires less energy than expected from the average tendency. This indicates that the deformation potential can be quite flat occasionally. Still, it is clear that approaching the coplanar equilibrium orientation, the torsional energy diminishes.

The partitioning of the energy barrier of the metallacycle formation into torsional (ΔG_{rot}) and chemical ($\Delta G^{\#}_{chem}$) terms (Fig. 2) affords translation of the effect of the possible steric repulsions to a factorized reaction rate expression using the transition state theory (TST).[23]

$$k = \frac{k_B T}{h} e^{\left(-\frac{\Delta G^{\#}}{RT}\right)} = \frac{k_B T}{h} e^{\left(-\frac{\Delta G_{rot} + \Delta G^{\#}_{chem}}{RT}\right)}$$
$$= e^{\left(-\frac{\Delta G_{rot}}{RT}\right)} \underbrace{\frac{k_B T}{h} e^{\left(-\frac{\Delta G^{\#}_{chem}}{RT}\right)}}_{k'} = \underbrace{e^{\left(-\frac{\Delta G_{rot}}{RT}\right)}}_{\text{prefactor}} k' \qquad (1)$$

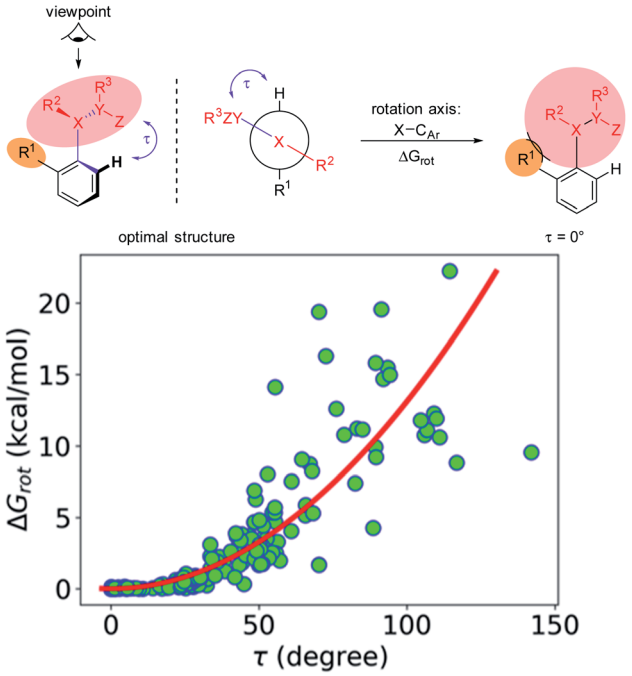

Fig. 3 Variation of the energy difference between the planar and equilibrium orientations of the DGs as a function of the deformational angle τ and its pictorial explanation. The red curve serves only as a guide.

Here k and k' are rate constants, $\Delta G^{\#}$ is the activation free energy and the sum of terms ΔG_{rot} and $\Delta G^{\#}_{chem}$; R is the universal gas constant, k_B is the Boltzmann constant, h is the Planck constant and T is the absolute temperature. k' can be interpreted as the hypothetical rate constant for the C–H activation step in the absence of any steric conflict during the metallacycle formation. The exponential prefactor $\exp(-\Delta G_{rot}/RT)$ can take a value between 0 and 1 and it expresses how easily the *ortho* substituent can assume the necessary conformation for the metallacycle. A value close to unity indicates a very small ΔG_{rot} (the substrate is predisposed for activation), while a small prefactor

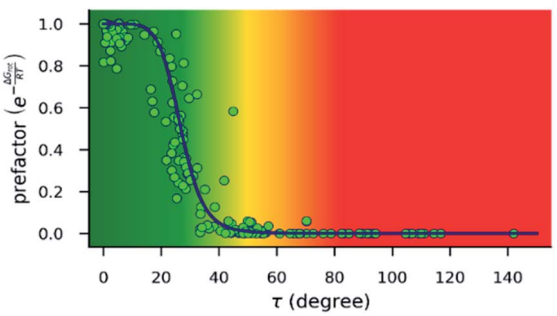

Fig. 4 Dependence of the exponential prefactor $\exp(-\Delta G_{rot}/RT)$ of eqn (1) on the torsional angle (τ) calculated for 25 °C. Note that this plot is a nonlinear transformation of the plot in Fig. 3. The blue line is only a guide. The background color gradient is an indication of the effect of torsion on the kinetics, *i.e.* it is a qualitative measure of the magnitude of the prefactor: green range: small effect is expected; red range: reaction is expected to be inhibited; yellow range: transient region.

© 2021 The Author(s). Published by the Royal Society of Chemistry

Open Access Article. Published on 02 March 2021. Downloaded on 9/25/2023 2:55:44 PM.
This article is licensed under a Creative Commons Attribution-NonCommercial 3.0 Unported Licence.

implies a large ΔG_{rot} and a reduced reactivity. Fig. 4 shows how this prefactor depends on the equilibrium torsional angle. A clear nonlinear behaviour can be seen. The shape of the curve is crucial for our model: the nonlinear dependence of the prefactor on τ results in a short plateau at small angles and a steep, almost linear decline to level off from $\tau \approx 60°$. It suggests that for torsional angles greater than $\approx 60°$ orders of magnitude slower rates can be expected as the prefactor is close to 0 and $\tau \approx 60°$ can be taken as a qualitative threshold separating the domains of expectedly efficient and inefficient reactions. It is worth noting that analogous factorizations of the rate expression can be given for other energy-barrier partitioning schemes.

Assessing the model

The next step in developing our reactivity model is to see whether there is correlation between the available experimental reaction performances and the calculated quantities (τ and ΔG_{rot}) of the substrates. The reactivity or reaction performance can be defined in a number of ways (rate, turnover frequency, yield, *etc.*), however there are two important issues to consider:

(I) Accurate kinetic measurements are seldom performed therefore experimental rates are not available; the only available information for deducing the reaction performance is the isolated yield. Consequently, our strategy is to employ the published yields as a measure of reactivity.[24] We note that using the experimental yields instead of accurate kinetic data limits the predictive power of our model because yields only qualitatively represent the reactivity. However, in default of kinetic data the yields are used with their limitations in mind.

(II) In order to cover the full range of reaction efficiencies we need both high and low reactivity cases. Still, the vast majority of the published reactions report good to excellent yields for well-known reasons, and low yields are rarely published, therefore data for low reactivities are taken mostly from our laboratory.

The energy necessary to reach the planar conformations (ΔG_{rot}) is meaningful if we know the reaction temperature. Indeed, the barrier of a given ΔG_{rot} is easier to overcome at higher temperature resulting in higher yield in a given reaction time. In order to take into account this effect, we have to express ΔG_{rot} in RT units (standardized ΔG_{rot}, $\Delta G'_{rot}$, a dimensionless quantity). $\Delta G'_{rot}$ indicates how much larger ΔG_{rot} is than the available thermal energy (RT), so it allows a meaningful comparison of the torsional hindrances for different temperatures. For example, if $\Delta G_{rot} = 5$ kcal mol^{-1}, the standardized $\Delta G'_{rot}$-s are 8.4 and 6.4 at 25 °C and 100 °C, respectively.[25] These values indicate that at higher temperatures the same calculated barrier represents a smaller hindrance. Fig. 5A and B show the yields as a function of torsional angles and $\Delta G'_{rot}$-s, respectively. Note that for these figures only those substrates were considered where experimental yields are available and the actual experimental temperatures were applied. Our first observation is that no clear correlation between the experimental yields and either the torsional angle τ or the standardized torsional energy can be detected in Fig. 5A and B. Still, a qualitative assessment can identify torsional angle or energy regions where we expect

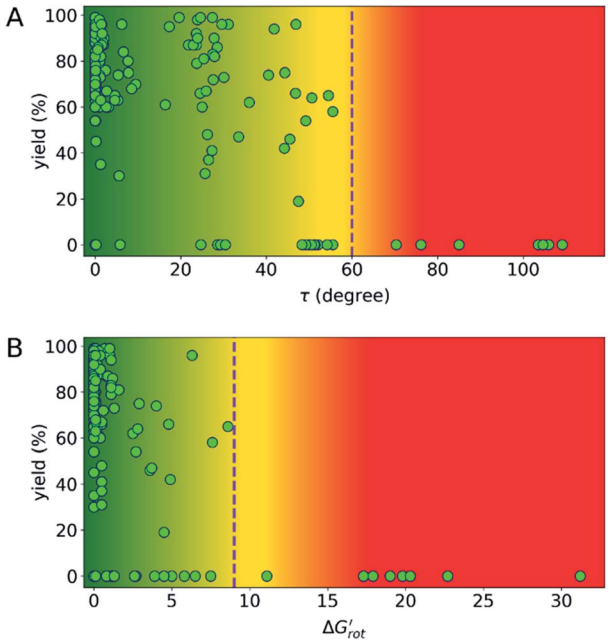

Fig. 5 (A) Variation of the experimental yield of a suitable Pd complex as a function of the torsional angle τ of the DGs. (B) Variation of the experimental yield of a suitable Pd complex as a function of the standardized conformational energy ($\Delta G_{rot}/RT$, $\Delta G'_{rot}$). The dashed lines separating reactive and unreactive substrates indicate thresholds which are discussed in the text later.

the reactions to occur (green and yellow regions) and the domain with larger torsional angle and energy values where reaction does not take place (indicated by the red background colour). To understand the origin of the peculiar scattering of the data points in Fig. 5A and B we recall that the outcome of a reaction is the function of both $\Delta G'_{rot}$ and $\Delta G^{\#}_{chem}$. Indeed, for a very favorable $\Delta G'_{rot}$ other factors (large $\Delta G^{\#}_{chem}$) can prevent a fast reaction and for a larger $\Delta G'_{rot}$ a reaction may be successful if the rest of the activation requires sufficiently small energy (small $\Delta G^{\#}_{chem}$).

This implies that scattering of the points is inevitable and it is more instructive to compare reactions where the term $\Delta G^{\#}_{chem}$ is expected to be very similar, *i.e.* for a given *ortho*-DG under similar conditions (see related calculations in the ESI,† where the contribution of the torsional energy ΔG_{rot} to the barrier is studied). However, data for successful and unsuccessful synthesis of palladacycles are limited, and consequently the number of data-points for a given DG is seldom sufficient to demonstrate the effect. These individual distributions are given in the ESI† displaying the variations of the yields as a function of τ and $\Delta G'_{rot}$ for the different classes of DGs.

At this point our goal is to obtain an overall insight. To this end, we turn to a more qualitative assessment of the available experimental and computational data. We define a substrate active if it can form an isolable palladacycle intermediate with a non-zero experimental yield. Fig. 6 shows the range of dihedral angle τ and computed $\Delta G'_{rot}$ for selected classes of *ortho*-DGs. These plots show all the available computational data for each class by means of the grey bars. Within a class, the ranges where

© 2021 The Author(s). Published by the Royal Society of Chemistry

Open Access Article. Published on 02 March 2021. Downloaded on 9/25/2023 2:55:44 PM.
This article is licensed under a Creative Commons Attribution-NonCommercial 3.0 Unported Licence.

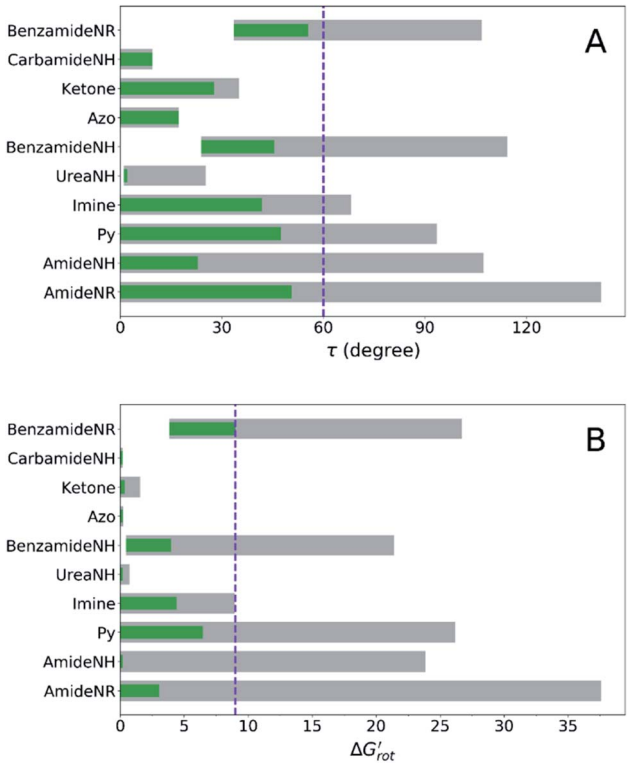

Fig. 6 (A) Range of the calculated torsional angle τ of the directing groups (green and grey bars). (B) Range of the standardized torsional energy ($\Delta G'_{rot}$) for the different DGs. The continuous green color in each bar indicates the range where non-zero experimental yield is available. For 'Azo' and 'Carbamide NH' the very narrow green range of $\approx$0.05 has been increased to $\approx$0.2 for better visibility.

non-zero experimental yields are available (active substrates) are indicated by green bars. Both figures show that depending on the nature of the DGs the range covered by computations can be quite wide. However, it is clearly seen that experimentally only those substrates are active and form palladacycle intermediates, whose dihedral angle τ and $\Delta G'_{rot}$ do not exceed specific thresholds ($\tau \approx 60°$ and $\Delta G'_{rot} \approx 9$) as also indicated by Fig. 5A and B respectively. Although the thresholds can be refined by adding additional future examples, the current overall picture also reveals finer details: for some DGs the ranges cover a wide possible torsional interval starting from fully planar equilibrium conformations, whereas for other DGs a non-negligible equilibrium torsion is always present implying considerable OE. However, not all reactive substrates form isolable palladacycles due to various reasons, hence it cannot be excluded that substrates outside the green regions might be reactive, although as we move upward to the larger values in a given class its probability diminishes sharply (*cf.* with Fig. 4).

Validation

Our theoretical model is designed to help synthetic chemists to design reactions and explain reactivities taking into account simple parameters such as τ, $\Delta G'_{rot}$ in such a way that the outcome of a C–H activation step can be explained on the basis of the actual values of these descriptors. Thus, the formation and stability of the corresponding palladacycle,[26] moreover the functionalizability of the substrate subjected to the Pd catalysed transformation can also be predicted (Fig. 7). Following this flowchart, we aimed to assess the validity of our model with the design of two sets of experiments.

In the first series of experiments, we selected substrates with similar anilide DG with a wide-range of the OE due to the varying extent of steric conflicts between the DG and the substituents next to the anilide chains. First we applied $Pd(OAc)_2$ catalyst in stoichiometric quantity and tested the reactivities of the substrates in forming palladacycles (Scheme 2). Note that the isolation of Pd complex intermediates is typical in mechanistic studies of C–H activation.

We found that 2-methylacetanilide (**1**), *N*-acetylindoline (**2**) and *N*-phenylpyrrolidin-2-one (**3**) underwent the palladation reaction and yielded the corresponding dimeric Pd complexes as yellow solids in 93%, 77% and 84% yields.[15] These results are in line with the calculated small torsional angles (0°, 2°, 24°) and small torsional energies ($\Delta G'_{rot} < 1$) indicating a negligible OE. In the case of *N*-acetyl tetrahydroquinoline (**4**) the equilibrium torsional angle is 44° ($\Delta G'_{rot} = 2.9$) and the corresponding Pd complex could be isolated in 75% yield. For substrates with larger torsional angles and torsional barriers (*N*-methylacetanilide (**5**), *N*-(2-tolyl)pyrrolydin-2-one (**6**)[27] and *N*-methyl-*N*-(2-tolyl)acetamide 7) isolation of the corresponding palladacycles failed even at 75 °C. Clearly, the efficiency of the complex formation follows

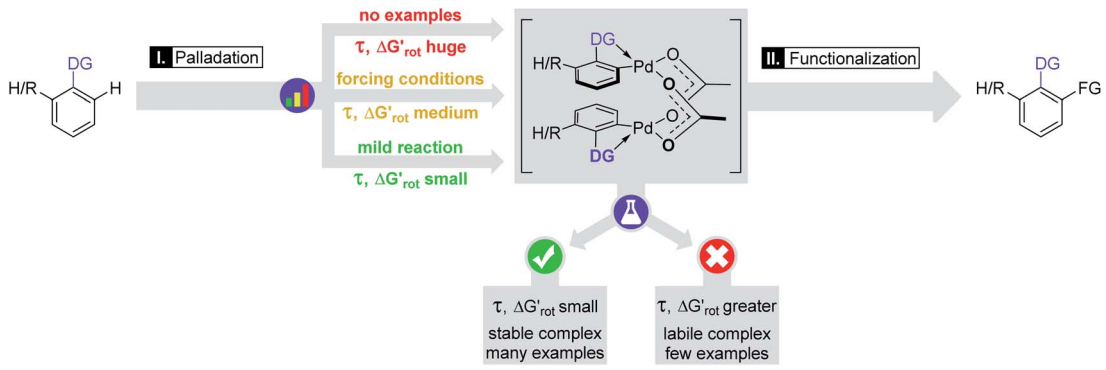

Fig. 7 Reactivity flowchart: synthetic approach for C–H palladation and direct functionalisation.

Open Access Article. Published on 02 March 2021. Downloaded on 9/25/2023 2:55:44 PM.
This article is licensed under a Creative Commons Attribution-NonCommercial 3.0 Unported Licence.

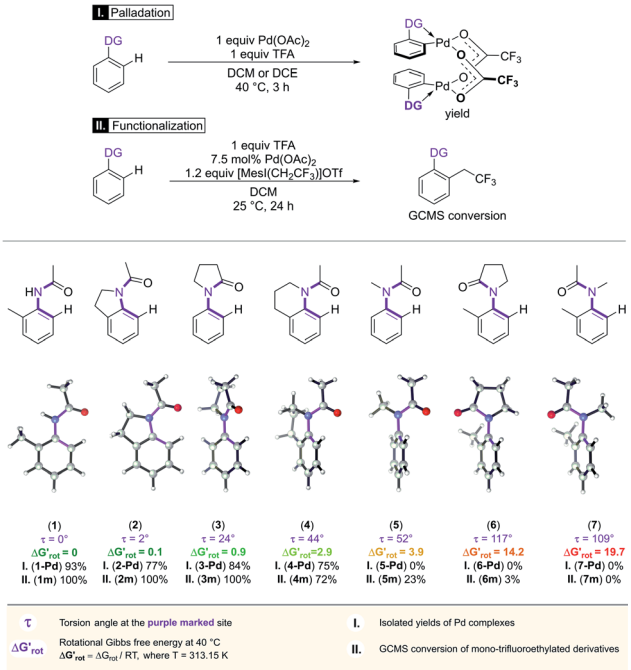

Scheme 2 The developing steric hindrance and ortho effect in aromatic amides.[29]

the trend predicted by the torsional angles and torsional barriers of the substrates. An important observation is that the OE is a joint action of both ligands interacting with each other. Indeed, taking substrates **1**, **6** and **7** as examples we can see that the methyl group in the *ortho* position does not necessarily signify OE (**1**), only if steric conflicts with the DG occur as in the case of substrates **6** and **7**.

We then performed Pd-catalysed trifluoroethylation reactions on the selected substrates as a straightforward and efficient C–H activation reaction, to show the correlation between the key physical parameters obtained from the model and the reaction efficiency (Scheme 2).[16] Performing a trifluoroethylation reaction on sterically less hindered substrates (**1**, **2**, **3**) with mesityl(trifluoroethyl)iodonium salt resulted in full conversion at 25 °C. However, the electrophilic trifluoroethylation of **4** provided 72% conversion under the same reaction conditions (25 °C, 24 h), which indicates a decreased reactivity shown by the somewhat larger τ and $\Delta G'_{rot}$ values (44°, 2.9). Curiously, although Pd complexes could not be obtained from substrates **5** and **6**, poor functionalisation could be achieved as shown by the yields (23% and 3%). This points to a reduced stability for the intermediate Pd complexes due to the non-planarity of the substrates which prevents their isolation. Finally, the highly distorted substrate **7** could not be functionalized, in agreement with the prediction of the model (very large τ torsional angle and $\Delta G^{\#}$ barrier height).

In the second set of experiments, we selected a site-selective DG on substrates with two linked aromatic rings, where competition between the anilide-like (**A**) and benzamide-like (**B**) sites is expected (Scheme 3),[28] and the outcome could be predicted on the basis of our model. Systematic variation of the OE could be achieved with strategical variation of the presence of a methyl group in *ortho* position to the amide-linker in both aryl-rings and on the amide-N. Again, we first applied $Pd(OAc)_2$ in stoichiometric amount to form palladacycles and subsequently we explored the reactivity of the substrates in the trifluoroethylation reaction and correlated the site-selectivities with the OE operating in the anilide and benzamide moieties.

The benzamide moiety forms a five-membered palladacycle, whereas the anilide unit results in a six-membered palladacycle. The model could successfully predict the regioselective outcome for both the Pd complexes and for the functionalisation experiments. We found that palladation of the core-scaffold *N*-phenylbenzamide (**8**) without any additional group on the phenyl rings occurred at the **A**-side, the corresponding Pd complex was isolated in 84% yield, and **B** remained unsubstituted. The trifluoroethylation of the same substrate resulted in full conversion and provided the monosubstituted product in 87% yield. This is in agreement with the smaller OE on the **A**-side as shown by the calculated torsional angles and barriers. A methyl group in the *ortho* position of anilide (**9**), benzamide (**10**) or both in **A** and **B** parts (**11**) did not modify either the regioselectivity or the reactivity, in accordance with the preserved smaller OE on **A**. The expected anilide-Pd complexes could be isolated in 67%, 85%, and 63% yields, respectively. In parallel,

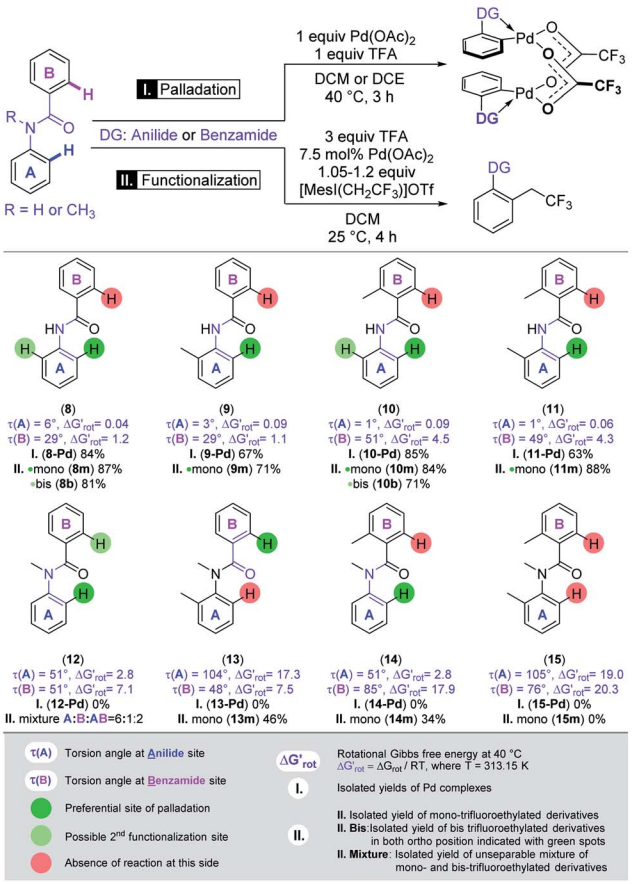

Scheme 3 The site-selectivity of methyl-substituted *N*-phenylbenzamides in C–H activation.

© 2021 The Author(s). Published by the Royal Society of Chemistry

Open Access Article. Published on 02 March 2021. Downloaded on 9/25/2023 2:55:44 PM.
This article is licensed under a Creative Commons Attribution-NonCommercial 3.0 Unported Licence.

the mono-trifluoroethylation of these substrates provided good and excellent yields (71%, 84%, 88%). By introducing a methyl group onto the linker amide-N (*N*-methyl-*N*-phenylbenzamide, **12**) we have found that both the *N*-methyl benzamide (**B**) and *N*-methyl anilide (**A**) moieties feature a considerable OE albeit of different extent. While the Pd complex could not be isolated, mono-trifluoroethylation of the substrate at room temperature took place on either **A** or **B** and both **AB** rings in an approximately 6 : 1 : 2 ratio (unseparable mixture) reflecting the more enhanced OE in the benzamide-moiety seen also in the theoretical descriptors. Further variation of the OE could be achieved by introducing additional methyl groups into the frame of compound **12**.

In this way, we studied the reactivity of all possible substrates (**13**, **14**, **15**). Similar to **12**, none of these compounds afforded the isolation of Pd complexes (presumably due to the considerable OE present in each side). Remarkably, the site-selectivity could be swapped in the case of **13** where a methyl group is introduced into ring **A**, leading to the *ortho*-trifluoroethylation of the benzamide side (**B**) and the corresponding product was isolated in 46% yield. This is again in very nice agreement with the prediction of our model, which indicated a prohibitively large OE on the **A**-side but forecasted moderate reactivity for the ring **B**.

The methyl group installed on ring **B** further increased the OE at this side as shown by the large torsional angles and barrier and this resulted in the *ortho*-trifluoroethylation of the anilide side **A** with a yield of 34%. Installation of a methyl group in ring **A** increased the OE at this side as well and substrate **15** is thus inactive in the Pd-catalysed functionalisation, in agreement with the predictions of our model, *i.e.* both descriptors indicate inactivity for both aromatic rings.

In substrates **8**, **10** and **14** two equivalent sites are available in the active ring **A** for *ortho*-functionalisation. Hence, we also tested if double equivalents of the trifluoroethyl reagent can afford the installation of two trifluoroethyl groups into the two *ortho* positions. We obtained bis-trifluoroethyl anilide **8b** in 81% yield and **10b** in 71% yield indicating only a moderate OE in mono-trifluoroethyl anilides **8m** and **10m**. In contrast, the bis-trifluoroethyl anilide **14b** could not be obtained which points to an amplified OE in **14m**.

In general, the steric hindrance and the OE of a functionalized arene can vary on a broad scale depending on the steric demands of the interacting groups.

General applicability and prediction

Beyond our designed experimental results in Scheme 4 we have collected a larger set of substrates along with the descriptors to quantify the extent of their OE to provide a more general picture of the applicability of the model. Herein we predict the possibility of successful functionalizations and the expected reaction temperatures in a pictorial way on the basis of the descriptors (for custom predictions use the attached Full Interactive Database equipped with Temperature Control Panel). We also indicate if literature precedents are available for such C–H functionalisation regardless of the incoming substituent.[30–46] In

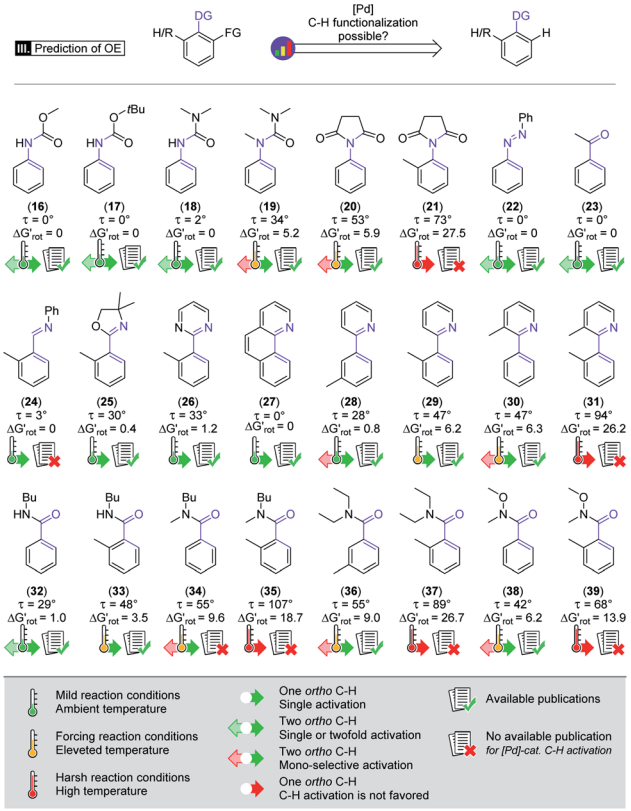

Scheme 4 Augmented demonstration and prediction of the steric repulsion and ortho effect. Values of $\Delta G'_{rot}$ are calculated at 25 °C.[30–46]

fact literature examples have not been found any of the substrates predicted to be unreactive. We have also considered bis-functionalisations when equivalent *ortho*-positions and sites are available. Similar to the aromatic NH amides, methyl phenylcarbamate (**16**), *tert*-butyl phenylcarbamate (**17**) and *N*,*N*-dimethyl-*N*′H-*N*′-phenylurea (**18**) feature coplanar structures and zero torsional energy which suggest mild reaction conditions and a possible twofold C–H activation, which are supported by experimental results.[30–32] However, the presence of an *N*-methyl group in *N*,*N*-dimethyl-*N*′-methyl-*N*′-phenylurea (**19**)[33] induces structural distortion and a larger $\Delta G'_{rot}$ implying a slower reaction. Hence, we propose an elevated reaction temperature. For substrates **16–18** bis-functionalisation is possible. However, its success is strongly dependent on the steric demand of the first substituent. Comparison of cyclic aromatic imide (**20**)[34] and its methylated variant **21** indicates a significant difference in the extent of the OE operating in the two substrates and **21** is predicted unreactive. There are known C–H activation reactions for azo and keto DGs such as **22** (ref. 35) and **23** (ref. 36) and the descriptors showing their planarity and also supporting their reactivity.

Similarly, only limited OE is predicted by the model for the nitrogen donor imines **24** and **25**,[37] for aromatic pyrimidine (**26**)[38] and for benzo[*h*]quinoline (**27**).[39]

These predictions are aided by the experimental examples from the literature. The development of the steric hindrance and how it tunes the OE is quite spectacular in the case of

Open Access Article. Published on 02 March 2021. Downloaded on 9/25/2023 2:55:44 PM.
This article is licensed under a Creative Commons Attribution-NonCommercial 3.0 Unported Licence.

phenyl pyridines: (**28**)[40] has a slightly twisted geometry typical of linked aryl rings and the CH_3 in the *meta* position is far from the DG. Hence the *ortho*-functionalisation is predicted to be feasible.

In addition, the success of a possible double functionalisation is again strongly dependent on the steric demand of the first installed substituent. The presence of *ortho*-methyl on either the aryl or pyridyl core (**29** and **30**)[41,42] typically makes the C–H activation difficult, as also indicated by the descriptors. To overcome this barrier, elevated temperature is proposed. For **30** a second *ortho*-substitution is also a possibility if the overall OE allows it. If both rings of the phenylpyridine frame have *o*-CH_3 (**31**) the torsional energy rises dramatically which might be compensated with harsh reaction conditions, although no literature precedent was found for the functionalisation of this substrate. Benzamides also feature an important DG in C–H activation reactions, although there are considerably less publications regarding their *ortho*-metalation reactions. The unsubstituted *N*-butyl benzamide (**32**)[43] has a slightly nonplanar geometry implying small OE and a feasible mono- and bis-functionalisation. Introducing a CH_3 group (**33**)[44] induces a larger OE and suggests a somewhat higher reaction temperature. Substrate pairs **34–35**, **36–37** and **38–39**[45,46] are good examples of how we can modify the OE by changing the interacting groups. For each pair we can see that the OE arising from the interaction of the alkyl groups on the amide-N moiety with the *ortho*-H atoms is considerable (**34**, **36**, **38**) but still within the productive range albeit indicating a reduced reactivity. Introduction of a larger group (**35**, **37**, **39**) however increases the OE, and further functionalisation in the *ortho* position is not feasible.

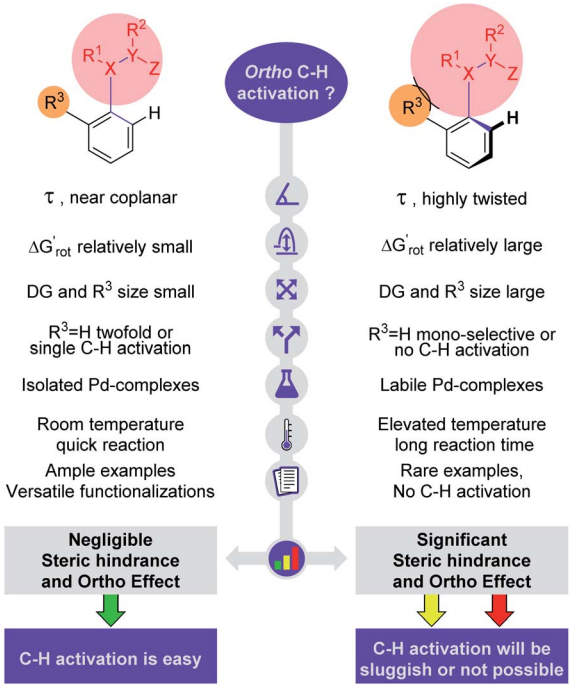

Fig. 8 Crucial parameters for the description of steric hindrance and OE in directing group (DG, shown by a red circle) supported C–H activation.

We note that increasing steric hindrance along the C–N axis can lead to restricted rotation and thus to the appearance of axial chirality.[47] Therefore, the substrates which will be functionalized with a larger group in the *ortho* position can be considered as axial prochiral substances and this structural property can be exploited in diverse synthetic approaches too.[48]

Conclusions

In this work we have introduced the concept of Ortho Effect (OE) in C–H activation. We can define it as the interaction between the directing group (DG) and an atom or a larger group installed in the *ortho* position relative to the DG, if this interaction influences the outcome of the directed C–H activation in the aromatic core in question. The present work has considered various *ortho*-DGs, where the effect is readily discernible and likely the most frequent as compared to *meta* and *para* DGs. Development of the model focused on the metallacycle formation step because usually it is rate-determining in C–H functionalisations under kinetic control. We sought descriptors representing the substrates alone which can predict their reactivities. The rotational angle of the DG and the corresponding rotational barrier were found to be such descriptors. An evident correlation between them has been found for a set of more than 250 substrates. Employing the transition state theory, we have shown how the rotational barrier can be translated to an overall rate decrease. In addition, we introduced a dimensionless quantity, the standardized rotational barrier which takes into account the experimental reaction temperature. To characterize the reactivities of the substrates we used the experimental yields. While it is true that using the experimental yields propagates their shortcomings to our reactivity model preventing a fully quantitative analysis, reactivity domains could be identified successfully with this approach. On this basis, useful thresholds for the practice could be set for the torsional angles and torsional barriers which can predict likely successful C–H activations, and in borderline cases allows estimation of a necessary reaction temperature. Indeed, with a torsional barrier ΔG_{rot} in hand one can estimate a minimal reaction temperature for a likely successful reaction from the fact that the threshold is for $\Delta G'_{rot} = \Delta G_{rot}/RT \lesssim 9$. Rearranging this relationship yields $T \gtrsim \Delta G_{rot}/9R$ setting a lower bound for the reaction temperature.

The model presented in this study provides a straightforward picture behind the OE. In a nutshell, if there is a coplanar or near coplanar arrangement formed by the aromatic ring and the sp^2 hybridized DG of substrates then the C–H activation can easily occur; highly twisted arrangement prevents a successful metallacycle formation.

In summary, the crucial elements of our model are depicted pictorially in Fig. 8. These elements are the torsion angle, conformational energy, size of DG and *ortho* substituent, stability of palladacycles, reaction temperature and number of literature precedents. The study also verified our hypothesis that the outcome of a C–H activation reaction can be assessed from the properties of the substrate alone. This analysis can be done with simple geometry optimizations and energy

© 2021 The Author(s). Published by the Royal Society of Chemistry

Open Access Article. Published on 02 March 2021. Downloaded on 9/25/2023 2:55:44 PM.
This article is licensed under a Creative Commons Attribution-NonCommercial 3.0 Unported Licence.

calculations of the substrate molecules without extensive quantum chemical calculations of the free energy profile of whole reaction mechanisms including the metal catalysts. We note that with properly tuned force fields one could calculate equilibrium torsional angles with the extremely fast and cheap molecular mechanics engines built in chemical drawing programs.

As a proof of concept, we have performed Pd-catalysed C–H functionalisations where the synthetic targets were strategically selected to verify the model. For a set of anilide compounds where differences between the electronic effects were minimized the correlations between the descriptors and reaction efficiencies were demonstrated. We have also shown how to apply the model to predict site-selectivity in functionalisations or how to tune mono *vs.* bis functionalisations. For a set of molecules, we have given a preliminary assessment of reactivity and selectivity in the functionalisations as well as reaction conditions on the basis of the model. We believe that our model can serve as a simple and useful tool for bench chemists and non-experts for a fast reactivity assessment in the field of *ortho*-directed C–H functionalisation.

Finally, we note that our database could be extended with further substrates and with the corresponding experimental and additional computed quantities. Including substrates showing moderate or no reactivities reported seldom in the literature would be highly useful and this provides additional argument favouring the publication of the so-called negative reactions. The value of such a database is that far better reactivity patterns could be obtained with more effective descriptors accounting for both reactive and unreactive situations. Certainly, modern machine learning tools could also be applied to such a sufficiently large database to obtain further suitable descriptors.

Conflicts of interest

There are no conflicts to declare.

Acknowledgements

This research was funded by the National Research, Development and Innovation Office (K116034 and K125120); this work was completed in the ELTE Thematic Excellence Programme 2020 supported by the National Research, Development and Innovation Office – TKP2020-IKA-05, and Cooperation Excellence Program with Research Centre for Natural Sciences, Eötvös Loránd Research Network. The research was supported by the EU and co-financed by the European Regional Development Fund under the project GINOP-2.3.2-15-2016-00008. The authors thank Ágnes Gömöry for the analytical measurements, and Dr P. P. Fehér at the Research Centre for Natural Sciences, Eötvös Loránd Research Network for fruitful discussions.

Notes and references

1 (*a*) Q. Zheng, C.-F. Liu, J. Chen and G.-W. Rao, *Adv. Synth. Catal.*, 2020, **362**, 1406; (*b*) P. Gandeepan, T. Müller, D. Zell, G. Cera, S. Warratz and L. Ackermann, *Chem. Rev.*, 2018, **119**, 2192; (*c*) C. Sambiagio, D. Schönbauer, R. Blieck, T. Dao-Huy, G. Pototschnig, P. Schaaf, T. Wiesinger, M. F. Zia, J. Wencel-Delord, T. Besset, B. U. W. Maes and M. Schnürch, *Chem. Soc. Rev.*, 2018, **47**, 6603; (*d*) Z. Dong, Z. Ren, S. J. Thompson, Y. Xu and G. Dong, *Chem. Rev.*, 2017, **117**, 9333; (*e*) L. Ping, D. S. Chung, J. Bouffard and S.-G. Lee, *Chem. Soc. Rev.*, 2017, **46**, 4299; (*f*) F. Roudesly, J. Oble and G. Poli, *J. Mol. Catal. A: Chem.*, 2017, **426**, 275; (*g*) B. Song and B. Xu, *Chem. Soc. Rev.*, 2017, **46**, 1103; (*h*) Y. Yang, J. Lan and J. You, *J. Chem. Rev.*, 2017, **117**, 8787–8863; (*i*) T. Gensch, M. N. Hopkinson, F. Glorius and J. Wencel-Delord, *Chem. Soc. Rev.*, 2016, **45**, 2900; (*j*) J. R. Hummel, J. A. Boerth and J. A. Ellman, *Chem. Rev.*, 2016, **117**, 9163; (*k*) C. Liu, J. Yuan, M. Gao, S. Tang, W. Li, R. Shi and A. Lei, *Chem. Rev.*, 2015, **115**, 12138; (*l*) S. H. Cho, J.-Y. Kim, J. Kwak and S. Chang, *Chem. Soc. Rev.*, 2011, **40**, 5068; (*m*) C. Liu, H. Zhang, W. Shi and A. Lei, *Chem. Rev.*, 2011, **111**, 1780; (*n*) J. Wencel-Delord, T. Dröge, F. Liu and F. Glorius, *Chem. Soc. Rev.*, 2011, **40**, 4740; (*o*) T. W. Lyons and M. S. Sanford, *Chem. Rev.*, 2010, **110**, 1147.

2 (*a*) Z. Chen, B. Wang, J. Zhang, W. Yu, Z. Liu and Y. Zhang, *Org. Chem. Front.*, 2015, **2**, 1107; (*b*) W. Ma, P. Gandeepan, J. Li and L. Ackermann, *Org. Chem. Front.*, 2017, **4**, 1435.

3 (*a*) G. Meng, N. Y. S. Lam, E. L. Lucas, T. G. Saint-Denis, P. Verma, N. Chekshin and J.-Q. Yu, *J. Am. Chem. Soc.*, 2020, **142**, 10571; (*b*) A. Gholap, S. Bag, S. Pradhan, A. R. Kapdi and D. Maiti, *ACS Catal.*, 2020, **10**, 5347; (*c*) L. Y. Liu, J. X. Qiao, K. S. Yeung, W. R. Ewing and J.-Q. Yu, *Angew. Chem., Int. Ed.*, 2020, **59**, 13831; (*d*) K. Korvorapun, M. Moselage, J. Struwe, T. Rogge, A. Messinis and L. Ackermann, *Angew. Chem., Int. Ed.*, 2020, **59**, 18795; (*e*) V. K. Tiwari and M. Kapur, *Org. Biomol. Chem.*, 2019, **17**, 1007; (*f*) A. Dey, S. Agasti and D. Maiti, *Org. Biomol. Chem.*, 2016, **14**, 5440; (*g*) C. J. Teskey, A. Y. W. Lui and M. F. Greaney, *Angew. Chem., Int. Ed.*, 2015, **54**, 11677; (*h*) Z. Dong, J. Wang and G. Dong, *J. Am. Chem. Soc.*, 2015, **137**, 5887; (*i*) J. Yang, *Org. Biomol. Chem.*, 2015, **13**, 1930; (*j*) Y.-J. Liu, H. Xu, W. J. Kong, M. Shang, H. X. Dai and J.-Q. Yu, *Nature*, 2014, **515**, 389; (*k*) J. Luo, S. Preciado and I. Larrosa, *J. Am. Chem. Soc.*, 2014, **136**, 4109; (*l*) R. J. Phipps and M. J. Gaunt, *Science*, 2009, **323**, 1593; (*m*) A. Dey, S. K. Sinha, T. K. Achar and D. Maiti, *Angew. Chem., Int. Ed.*, 2019, **58**, 10820; (*n*) S. Porey, X. Zhang, S. Bhowmick, V. K. Singh, S. Guin, R. S. Paton and D. Maiti, *J. Am. Chem. Soc.*, 2020, **142**, 3762.

4 (*a*) U. Dutta, S. Porey, S. Pimparkar, A. Mandal, J. Grover, A. Koodan and D. Maiti, *Angew. Chem., Int. Ed.*, 2020, **59**, 20831; (*b*) M. T. Mihai, B. D. Williams and R. J. Phipps, *J. Am. Chem. Soc.*, 2019, **141**, 15477; (*c*) U. Dutta, S. Maiti, S. Pimparkar, S. Maiti, L. R. Gahan, E. H. Krenske, D. W. Lupton and D. Maiti, *Chem. Sci.*, 2019, **10**, 7426; (*d*) K. Naksomboon, J. Poater, F. M. Bickelhaupt and M. Á. Fernández-Ibáñez, *J. Am. Chem. Soc.*, 2019, **141**, 6719; (*e*) T. Patra, S. Bag, R. Kancherla, A. Mondal, A. Dey, S. Pimparkar, S. Agasti, A. Modak and D. Maiti, *Angew. Chem., Int. Ed.*, 2016, **55**, 7751; (*f*) G. Tu, C. Yuan, Y. Li,

Open Access Article. Published on 02 March 2021. Downloaded on 9/25/2023 2:55:44 PM. This article is licensed under a Creative Commons Attribution-NonCommercial 3.0 Unported Licence.

J. Zhang and Y. Zhao, *Angew. Chem., Int. Ed.*, 2018, **57**, 15597; (*g*) C. Yuan, L. Zhu, C. Chen, X. Chen, Y. Yang, Y. Lan and Y. Zhao, *Nat. Commun.*, 2018, **9**, 1189; (*h*) S. Bag, T. Patra, A. Modak, A. Deb, S. Maity, U. Dutta, A. Dey, R. Kancherla, A. Maji, A. Hazra, M. Bera and D. Maiti, *J. Am. Chem. Soc.*, 2015, **137**, 11888.

5 (*a*) D. Lapointe and K. Fagnou, *Chem. Lett.*, 2010, **39**, 1118; (*b*) Y. Boutadla, D. L. Davies, S. A. Macgregor and A. I. Poblador-Bahamonde, *Dalton Trans.*, 2009, **30**, 5820; (*c*) D. Stuart and K. Fagnou, *Science*, 2007, **316**, 1172; (*d*) D. L. Davies, S. M. A. Donald and S. A. Macgregor, *J. Am. Chem. Soc.*, 2005, **127**, 13754; (*e*) S. A. Kurzeev, G. M. Kazankov and A. D. Ryabov, *Inorg. Chim. Acta*, 2002, **340**, 192; (*f*) A. D. Ryabov, *Chem. Rev.*, 1990, **90**, 403–424.

6 (*a*) D. García-Cuadrado, P. de Mendoza, P. A. A. C. Braga, F. Maseras and A. M. Echavarren, *J. Am. Chem. Soc.*, 2007, **129**, 6880; (*b*) J.-R. Wang, C.-T. Yang, L. Liu and Q.-X. Guo, *Tetrahedron Lett.*, 2007, **48**, 5449; (*c*) L.-C. Campeau, M. Parisien, M. Leblanc and K. Fagnou, *J. Am. Chem. Soc.*, 2004, **126**, 9186; (*d*) J. J. González, N. García, B. Gómez-Lor and A. M. Echavarren, *J. Org. Chem.*, 1997, **62**, 1286.

7 H. Horino and N. Inoue, *J. Org. Chem.*, 1981, **46**, 4416.

8 W. Mossi, A. J. Klaus and P. Rys, *Helv. Chim. Acta*, 1992, **75**, 2531.

9 F. Yang, F. Song, W. Li, J. Lan and J. You, *RSC Adv.*, 2013, **3**, 9649.

10 S. J. Tremont and H. U. Rahman, *J. Am. Chem. Soc.*, 1984, **106**, 5759.

11 M. D. K. Boele, G. P. F. van Strijdonck, A. H. M. de Vries, P. C. J. Kamer, J. G. de Vries and P. W. N. M. van Leeuwen, *J. Am. Chem. Soc.*, 2002, **124**, 1586.

12 V. G. Zaitsev and O. Daugulis, *J. Am. Chem. Soc.*, 2005, **127**, 4156.

13 B. S. Kim, C. Jang, D. J. Lee and S. W. Youn, *Chem.–Asian J.*, 2010, **5**, 2336.

14 M. Tobisu, Y. Ano and N. Chatani, *Org. Lett.*, 2009, **11**, 3250.

15 C. S. Yeung, X. Zhao, N. Borduas and V. M. Dong, *Chem. Sci.*, 2010, **1**, 331.

16 B. L. Tóth, S. Kovács, G. Sályi and Z. Novák, *Angew. Chem., Int. Ed.*, 2016, **55**, 1988.

17 B. P. Mathew, H. J. Yang, J. Kim, J. B. Lee, Y.-T. Kim, S. Lee, C. Y. Lee, W. Choe, K. Myung, J.-U. Park and S. Y. Hong, *Angew. Chem., Int. Ed.*, 2017, **56**, 5007.

18 (*a*) A. V. Brethomé, S. P. Fletcher and R. S. Paton, *ACS Catal.*, 2019, **9**, 2313; (*b*) J. P. Reid and M. S. Sigman, *Nature*, 2019, **571**, 343.

19 (*a*) D. J. Durand and N. Fey, *Chem. Rev.*, 2019, **119**, 6561; (*b*) M. Foscato and V. R. Jensen, *ACS Catal.*, 2020, **10**, 2354.

20 M. J. Frisch*et al.Gaussian 09, Revision E.01*, Gaussian, Inc., Wallingford CT, 2013.

21 J.-D. Chai and M. Head-Gordon, *Phys. Chem. Chem. Phys.*, 2008, **10**, 6615.

22 (*a*) F. M. Bickelhaupt and K. N. Houk, *Angew. Chem., Int. Ed.*, 2017, **56**, 10070; (*b*) D. H. Ess and K. N. Houk, *J. Am. Chem. Soc.*, 2008, **130**, 10187; (*c*) F. M. Bickelhaupt, *J. Comput. Chem.*, 1999, **20**, 114.

23 E. Pollak and P. Talkner, *Chaos*, 2005, **15**, 26116.

24 Discussion of a possible standardization of the published yields is given in the ESI.†

25 Note that the Gibbs free energy is a temperature dependent quantity but we neglect this dependence in this study.

26 B. E. Haines, J. F. Berry, J.-Q. Yu and D. G. Musaev, *ACS Catal.*, 2016, **6**, 829.

27 D. G. Billing, J. C. A. Boeyens, L. Denner, K. E. D. Plooy, G. C. Long and J. P. Michael, *Acta Crystallogr.*, 1991, **47**, 284.

28 (*a*) Q. Lin, Z. Lin, M. Pan, Q. Zheng, H. Li, X. Chen, C. Darcel, P. H. Dixneuf and B. Li, *Org. Chem. Front.*, 2021, **8**, 514–521; (*b*) K. Sahoo, P. Pradhan and N. Panda, *Org. Biomol. Chem.*, 2020, **18**, 1820; (*c*) R. Gramage-Doria, *Chem.–Eur. J.*, 2020, **26**, 9688; (*d*) A. Tomberg, M. É. Muratore, M. J. Johansson, I. Terstiege, C. Sköld and P.-O. Norrby, *iScience*, 2019, **20**, 373; (*e*) Y.-H. Sun, T.-Y. Sun, Y.-D. Wu, X. Zhang and Y. Rao, *Chem. Sci.*, 2016, **7**, 2229.

29 C. Y. Legault, *The optimized structures were visualized with CYLview, 1.0b*, Université de Sherbrooke, 2009, http://www.cylview.org.

30 (*a*) Q.-L. Li, Z.-Y. Li and G.-W. Wang, *ACS Omega*, 2018, **3**, 4187; (*b*) A. Polley, K. Varalaxmi and R. Jana, *ACS Omega*, 2018, **3**, 14503; (*c*) N. Uhlig and C.-J. Li, *Chem.–Eur. J.*, 2014, **20**, 12066.

31 E. Dubost, V. Babin, F. Benoist, A. Hebert, P. Barbey, C. Chollet, J.-P. Bouillon, A. Manrique, G. Pieters, F. Fabis and T. Cailly, *Org. Lett.*, 2018, **20**, 6302.

32 (*a*) S. Kovács, B. L. Tóth, G. Borsik, T. Bihari, N. V. May, A. Stirling and Z. Novák, *Adv. Synth. Catal.*, 2017, **359**, 527; (*b*) T. Nishikata, A. R. Abela, S. Huang and B. H. Lipshutz, *Beilstein J. Org. Chem.*, 2016, **12**, 1040; (*c*) C. E. Houlden, M. Hutchby, C. D. Bailey, J. G. Ford, S. N. G. Tyler, M. R. Gagne, G. C. Lloyd-Jones and K. I. Booker-Milburn, *Angew. Chem., Int. Ed.*, 2009, **48**, 1830.

33 Z. Jiang, L. Zhang, C. Dong, X. Su, H. Li, W. Tang, L. Xu and Q. Fan, *RSC Adv.*, 2013, **3**, 1025.

34 C. Zhang, Y. Song, Z. Sang, L. Zhan and Y. Rao, *J. Org. Chem.*, 2018, **83**, 2582.

35 (*a*) G. Hong, D. Mao, S. Wu and L. Wang, *J. Org. Chem.*, 2014, **79**, 10629; (*b*) X.-T. Ma and S.-K. Tian, *Adv. Synth. Catal.*, 2013, **355**, 337; (*c*) H. Li, P. Li, H. Tan and L. Wang, *Chem.–Eur. J.*, 2013, **19**, 14432.

36 G. Shan, X. Yang, L. Ma and Y. Rao, *Angew. Chem., Int. Ed.*, 2012, **51**, 13070.

37 D. A. Gutierrez, W.-C. C. Lee, Y. Shen and J. J. Li, *Tetrahedron Lett.*, 2016, **57**, 5372.

38 (*a*) X. Wang, L. Truesdale and J.-Q. Yu, *J. Am. Chem. Soc.*, 2010, **132**, 3648; (*b*) Q.-L. Yang, C.-Z. Li, L.-W. Zhang, Y.-Y. Li, X. Tong, X.-Y. Wu and T.-S. Mei, *Organometallics*, 2019, **38**, 1208.

39 (*a*) D. C. Powers and T. Ritter, *Nat. Chem.*, 2009, **1**, 302; (*b*) Q.-Y. Han, X. Hu, X.-S. Xue, C.-L. Zhao and C.-P. Zhang, *Asian J. Org. Chem.*, 2019, **8**, 665.

40 (*a*) X. Wang, X. Ji, C. Shao, Y. Zhang and Y. Zhang, *Org. Biomol. Chem.*, 2017, **15**, 5616; (*b*) A. Hossian, M. K. Manna, K. Manna and R. Jana, *Org. Biomol. Chem.*, 2017, **15**, 6592; (*c*) D. Kalyani and M. S. Sanford, *Org. Lett.*, 2005, **7**, 4149.

© 2021 The Author(s). Published by the Royal Society of Chemistry

Open Access Article. Published on 02 March 2021. Downloaded on 9/25/2023 2:55:44 PM.
This article is licensed under a Creative Commons Attribution-NonCommercial 3.0 Unported Licence.

41 (*a*) S. R. Neufeldt, C. K. Seigerman and M. S. Sanford, *Org. Lett.*, 2013, **15**, 2302; (*b*) X. Wang, X. Ji, C. Shao, Y. Zhang and Y. Zhang, *Org. Biomol. Chem.*, 2017, **15**, 5616.

42 (*a*) D. Kalyani, N. R. Deprez, L. V. Desai and M. S. Sanford, *J. Am. Chem. Soc.*, 2005, **127**, 7330; (*b*) X. Chen, C. E. Goodhue and J.-Q. Yu, *J. Am. Chem. Soc.*, 2006, **128**, 12634; (*c*) C. K. Seigerman, T. M. Micyus, S. R. Neufeldt and M. S. Sanford, *Tetrahedron*, 2013, **69**, 5580.

43 M. Maraswami, S. Pankajakshan, G. Chen and T.-P. Loh, *Org. Lett.*, 2017, **19**, 4223.

44 C. Luis and N. C. Misal Castro, *Chem.–Eur. J.*, 2014, **20**, 4548.

45 (*a*) K. Jing, J.-P. Yao, Z.-Y. Li, Q.-L. Li, H.-S. Lin and G.-W. Wang, *J. Org. Chem.*, 2017, **82**, 12715; (*b*) F.-C. Qiu, W.-C. Yang, Y.-Z. Chang and B.-T. Guan, *Asian J. Org. Chem.*, 2017, **6**, 1361.

46 (*a*) R. Das and M. Kapur, *J. Org. Chem.*, 2017, **82**, 1114; (*b*) Y. Wang, K. Zhou, Q. Lan and X.-S. Wang, *Org. Biomol. Chem.*, 2015, **13**, 353.

47 (*a*) J. E. Díaz, A. Mazzanti, L. R. Orelli and M. Mancinelli, *ACS Omega*, 2019, **4**, 4712; (*b*) A. Iida, M. Matsuoka, H. Hasegawa, N. Vanthuyne, D. Farran, C. Roussel and O. Kitagawa, *J. Org. Chem.*, 2019, **84**, 3169; (*c*) E. Bisz, A. Piontek, B. Dziuk, R. Szostak and M. Szostak, *J. Org. Chem.*, 2018, **83**, 3159; (*d*) K. T. Barrett, A. J Metrano, P. R. Rablen and S. J. Miller, *Nature*, 2014, **509**, 71; (*e*) S. R. LaPlante, P. J. Edwards, L. D. Fader, A. Jakalian and O. Hucke, *ChemMedChem*, 2011, **6**, 505; (*f*) J. Clayden, *Chem. Commun.*, 2004, **2**, 127; (*g*) A. Ahmed, R. A. Bragg, J. Clayden, L. W. Lai, C. McCarthy, J. H. Pink, N. Westlund and S. A. Yasin, *Tetrahedron*, 1998, **54**, 13277.

48 (*a*) M. I. Lapuh, S. Mazeh and T. Besset, *ACS Catal.*, 2020, **10**, 12898; (*b*) R. Costil, A. J. Sterling, F. Duarte and J. Clayden, *Angew. Chem., Int. Ed.*, 2020, **59**, 18670; (*c*) Q.-J. Yao, P.-P. Xie, Y.-J. Wu, Y.-L. Feng, M.-Y. Teng, X. Hong and B.-F. Shi, *J. Am. Chem. Soc.*, 2020, **142**, 18266; (*d*) H. Li, X. Yan, J. Zhang, W. Guo, J. Jiang and J. Wang, *Angew. Chem., Int. Ed.*, 2019, **58**, 6732; (*e*) Q. Dherbassy, J.-P. Djukic, J. Wencel-Delord and F. Colobert, *Angew. Chem., Int. Ed.*, 2018, **57**, 4668; (*f*) Q.-Y. Sun, W.-Y. Ma, K.-F. Yang, J. Cao, Z.-J. Zheng, Z. Xu, Y.-M. Cui and L.-W. Xu, *Chem. Commun.*, 2018, **54**, 10706; (*g*) S.-X. Li, Y.-N. Ma and S.-D. Yang, *Org. Lett.*, 2017, **19**, 1842–1845.

© 2021 The Author(s). Published by the Royal Society of Chemistry